

Thermodynamics, Molecular Mobility and Crystallization Kinetics of Amorphous Griseofulvin

Deliang Zhou,[†] Geoff G. Z. Zhang,[†] Devalina Law,[‡] David J. W. Grant,[§] and Eric A. Schmitt^{*†}

Global Pharmaceutical R&D, and Global Pharmaceutical Operations, Abbott Laboratories, and Department of Pharmaceutics, College of Pharmacy, University of Minnesota, Weaver-Densford Hall, 308 Harvard Street SE, Minneapolis, Minnesota 55455-0343

Received September 16, 2008; Revised Manuscript Received October 13, 2008; Accepted October 14, 2008

Abstract: Griseofulvin is a small rigid molecule that shows relatively high molecular mobility and small configurational entropy in the amorphous phase and tends to readily crystallize from both rubbery and glassy states. This work examines the crystallization kinetics and mechanism of amorphous griseofulvin and the quantitative correlation between the rate of crystallization and molecular mobility above and below T_g . Amorphous griseofulvin was prepared by rapidly quenching the melt in liquid N_2 . The thermodynamics and dynamics of amorphous phase were then characterized using a combination of thermal analysis techniques. After characterization of the amorphous phase, crystallization kinetics above T_g were monitored by isothermal differential scanning calorimetry (DSC). Transformation curves for crystallization fit a second-order John–Mehl–Avrami (JMA) model. Crystallization kinetics below T_g were monitored by powder X-ray diffraction and fit to the second-order JMA model. Activation energies for crystallization were markedly different above and below T_g suggesting a change in mechanism. In both cases molecular mobility appeared to be partially involved in the rate-limiting step for crystallization, but the extent of correlation between the rate of crystallization and molecular mobility was different above and below T_g . A lower extent of correlation below T_g was observed which does not appear to be explained by the molecular mobility alone and the diminishing activation energy for crystallization suggests a change in the mechanism of crystallization.

Keywords: Amorphous; crystallization; griseofulvin; John–Mehl–Avrami (JMA); molecular mobility; nucleation; stability

Introduction

Amorphous pharmaceuticals have attracted significant research due to their potential for improving dissolution rate of the increasing number of poorly water-soluble drug candidates. Despite progress in recent years, one of the main

challenges of developing amorphous pharmaceuticals is the fundamental understanding and therefore the predictability of physical and chemical stability of amorphous phases.^{1,2} Molecular mobility is generally thought to be a key factor

* Author to whom correspondence should be addressed. Mailing address: Abbott Laboratories, 1401 Sheridan Road, Dept. R4P7, Bldg. M3B, North Chicago, IL 60064-6246. Tel: (847) 938-4835. Fax: (847) 937-8918. E-mail: eric.a.schmitt@abbott.com.

[†] Global Pharmaceutical R&D, Abbott Laboratories.

[‡] Global Pharmaceutical Operations, Abbott Laboratories.

[§] University of Minnesota.

- (1) Pikal, M. J.; Lukes, A. L.; Lang, J. E.; Gaines, K. Quantitative crystallinity determinations for β -lactam antibiotics by solution calorimetry: Correlations with stability. *J. Pharm. Sci.* **1978**, *67*, 767–772.
- (2) Aso, Y.; Yoshioka, S.; Otsuka, T.; Kojima, S. The physical stability of amorphous nifedipine determined by isothermal microcalorimetry. *Chem. Pharm. Bull.* **1995**, *43*, 300–303.
- (3) Hancock, B. C.; Shamblin, S. L.; Zografi, G. Molecular mobility of amorphous pharmaceutical solids below their glass transition temperature. *Pharm. Res.* **1995**, *12*, 799–806.

governing the stability of amorphous phases^{3,4} and has been the subject of many studies.^{5–8} For example, molecular mobility has been shown to partially correlate with the physical⁸ and chemical⁹ stability of a few amorphous pharmaceuticals. However, other reports have suggested the contribution of molecular mobility to stability was negligible.^{10,11}

Thermodynamic factors such as configurational entropy have been shown to contribute to the physical stability of amorphous pharmaceuticals. Previously, we have presented cases where both molecular mobility and configurational entropy were important in determining the crystallization tendency from the rubbery state.¹² Similar observations were later made for glassy pharmaceuticals.¹³ We have hypothesized that the configurational entropy, as estimated by calorimetry, is inversely related to the probability of the molecules being in the appropriate conformation for nucleation and crystallization.

In this study, we characterize the amorphous phase of griseofulvin (Figure 1), examine crystallization kinetics and mechanism and finally attempt to draw a quantitative correlation between the crystallization rate, and molecular mobility at temperatures above and below the glass transition temperature.

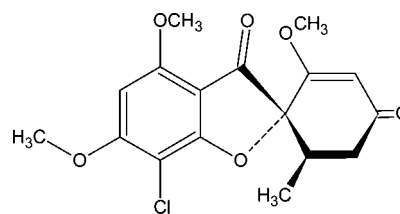


Figure 1. Structure of griseofulvin.

Experimental Section

Material. Griseofulvin (>99%), obtained from Sigma Chemical Corporation (Saint Louis, MO) as a white powder, was used without further purification.

Differential Scanning Calorimetry (DSC). DSC experiments were performed using a modulated DSC (MDSC 2920, TA Instruments, New Castle, DE) equipped with a refrigerated cooling accessory (RCS) and a data analyzer (Universal Analysis, version 2.5, TA Instruments). In all experiments, the DSC cell was purged with nitrogen at 50 mL/min. Indium was used to calibrate the cell constant. A four-point temperature calibration was constructed from the melting points of water, biphenyl, indium, and tin. Heat capacity measurements for amorphous and crystalline griseofulvin were carried out using MDSC in hermetically sealed pans under the following conditions: underlying heating rate of 1 °C/min, modulation amplitude of 0.5 °C, and modulation period of 100 s. Additional experimental details can be found elsewhere.¹²

Heating Rate Dependence of the Glass Transition Temperature. The heating rate dependence of the glass transition temperature was determined for amorphous griseofulvin using a Q-1000 DSC equipped with a liquid nitrogen cooling system (LNCS) (TA Instruments, New Castle, DE) at heating rates of 1, 2, 5, 10, 15, 20, 30, 40 and 50 °C/min. Prior to heating, the sample was cooled from a temperature well above T_g to temperatures below T_g at a rate identical to the subsequent heating rate.^{14,15}

Powder X-ray Diffractometry (PXRD). The diffractometer (XDS 2000, Scintag, Sunnyvale, CA) consisted of a 4 kW generator (voltage 45 kV and current 40 mA) with Cu K α radiation, with a liquid-nitrogen-cooled Ge detector (GLP-10195/07-S, EG&G ORTEC, Oak Ridge, TN) and data analyzer (DMSNT Data Analysis, version 1.27, Scintag). The samples were packed into stainless steel holders and scanned while spinning at a step size of 0.02° with a dwell time of 1.2 s.

Hot Stage Microscopy (HSM). Visual changes during crystallization were observed using a polarizing microscope (Eclipse E600POL, Nikon, Melville, NY) equipped with a hot stage (FP82HT stage and FP90 processor, Mettler Instruments, Hightstown, NJ).

- (4) Hancock, B. C.; Zografi, G. Characteristics and significance of the amorphous state in pharmaceutical systems. *J. Pharm. Sci.* **1997**, *86*, 1–12.
- (5) Duddu, S. P.; Zhang, G.; Dal Monte, P. R. The relationship between protein aggregation and molecular mobility below the glass transition temperature of lyophilized formulations containing a monoclonal antibody. *Pharm. Res.* **1997**, *14*, 596–600.
- (6) Shamblin, S. L.; Tang, X.; Chang, L.; Hancock, B. C.; Pikal, M. J. Characterization of the time scales of molecular motion in pharmaceutically important glasses. *J. Phys. Chem.* **1999**, *103B*, 4113–4121.
- (7) Yoshioka, S.; Aso, Y.; Kojima, S. Temperature dependence of bimolecular reactions associated with molecular mobility in lyophilized formulations. *Pharm. Res.* **2000**, *17*, 925–929.
- (8) Aso, Y.; Yoshioka, S.; Kojima, S. Explanation of the crystallization rate of amorphous nifedipine and phenobarbital from their molecular mobility as measured by ¹³C nuclear magnetic resonance relaxation time and the relaxation time obtained from the heating rate dependence of the glass transition temperature. *J. Pharm. Sci.* **2001**, *90*, 798–806.
- (9) Guo, Y.; Byrn, S. R.; Zografi, G. Physical characteristics and chemical degradation of amorphous quinapril hydrochloride. *J. Pharm. Sci.* **2000**, *89*, 128–143.
- (10) Yoshioka, S.; Aso, Y. A quantitative assessment of the significance of molecular mobility as a determinant for the stability of lyophilized insulin formulation. *Pharm. Res.* **2005**, *22*, 1358–1364.
- (11) Yoshioka, S.; Aso, Y.; Miyazaki, T. Negligible contribution of molecular mobility to the degradation rate of insulin lyophilized with poly(vinylpyrrolidone). *J. Pharm. Sci.* **2006**, *95*, 939–43.
- (12) Zhou, D.; Zhang, G. G. Z.; Law, D.; Grant, D. J. W.; Schmitt, E. A. Physical stability of amorphous pharmaceuticals: Importance of configurational thermodynamic quantities and molecular mobility. *J. Pharm. Sci.* **2002**, *91*, 1863–1872.
- (13) Zhou, D.; Grant, D. J. W.; Zhang, G. G. Z.; Law, D.; Schmitt, E. A. A calorimetric investigation of thermodynamic and molecular mobility contributions to the physical stability of two pharmaceutical glasses. *J. Pharm. Sci.* **2007**, *96*, 71–83.

- (14) Moynihan, C. T.; Easteal, A. J.; Wilder, J.; Tucker, J. Dependence of the glass transition temperature on heating and cooling rate. *J. Phys. Chem.* **1974**, *78*, 2673–2677.
- (15) Moynihan, C. T.; S.-K., L.; Tatsumisago, M.; Minami, T. Estimation of activation energies for structural relaxation and viscous flow from DTA and DSC experiments. *Thermochim. Acta* **1996**, *280–281*, 153–162.

High Performance Liquid Chromatography (HPLC). HPLC was performed on a system consisting of a ternary pump (SP 8800-010, Spectra-Physics, San Jose, CA), an autosampler (AS4000, Hitachi Instruments, Danbury, CT), a programmable ultraviolet (UV) detector (at 254 nm, model 783A, Applied Biosystems, Foster City, CA), and a data acquisition system (PeakPro version 8.3.1, Beckman Instruments, Fullerton, CA). The mobile phase consisted of water/methanol (65:35 v/v), which was pumped through a Zorbax CN column at a flow rate of 1.0 mL/min. The method was modified from Townley and Roden.¹⁶

Isothermal Crystallization above the Glass Transition Temperature. About 10 mg of crystalline griseofulvin powder was packed into a hermetically sealed DSC pan, and heated until molten. After the fusion was complete (5 min at 223 °C), the DSC pan was quickly quenched in liquid nitrogen. The amorphous sample obtained was then held isothermally at 115, 120, 123, 125, 130, 134, and 139 °C. The heat flow evolved during each crystallization experiment was monitored directly by DSC.

Crystallization at and below the Glass Transition Temperature. Crystallization kinetics of amorphous griseofulvin at 90, 75, and 60 °C were monitored using PXRD. A tablet containing about 0.12 g of griseofulvin was placed into a stainless steel sample holder, which was then melted in an oven at 223 °C and quenched in liquid nitrogen. The resulting amorphous samples were stored in ovens at 90, 75, and 60 °C. Their PXRD patterns were determined at various time intervals. At each time interval, the same sample of alpha-alumina as an external standard was also scanned, in order to correct for the fluctuations in detector responses. The total intensities of the four peaks, 10.9, 13.4, 14.7, and 16.6° 2 θ , were normalized to the intensity of the external standard and used for quantitative analysis. At the end of each study, the samples were made to fully crystallize by holding at 135 °C for 3 h. The fractional conversion, α , was then calculated as

$$\alpha = I(t)/I_{\infty} \quad (1)$$

where $I(t)$ is the integrated peak intensity for the sample at time t and I_{∞} is that for the fully crystallized sample, both normalized with the external standard.

Non-Isothermal Crystallization. Amorphous griseofulvin was prepared in a DSC pan in the same way as in the isothermal studies. Amorphous samples were then heated at 1, 2, 5, 10, 15, and 20 °C/min to 225 °C, just above its melting temperature.

Non-Isothermal Crystallization of the Seeded Sample. A powdered sample of amorphous griseofulvin was blended with 10% (w/w) crystalline griseofulvin. The blend was subdivided, placed in DSC pans and scanned at linear heating rates indicated for non-isothermal crystallization.

Theoretical Background

Thermodynamics. Excess thermodynamic quantities of the amorphous phase can be obtained from heat capacity data via the standard thermodynamic treatments.¹²

Molecular Mobility. Molecular mobility, which is the common term for the reciprocal of relaxation time constant (τ), was calculated based on the Adam–Gibbs model:

$$\tau = \tau_0 \exp\left(\frac{C}{TS_c}\right) \quad (2)$$

where τ is molecular relaxation time constant, τ_0 is a constant ($\sim 10^{-14}$ second), T is the absolute temperature, S_c is the configurational entropy, and C is a material dependent constant. Strictly speaking, configurational entropy refers to the entropy difference between the amorphous and crystalline states due to the differences in the number of configurations. In this study, the excess entropy between the amorphous and crystalline phase was taken as an estimate of the configurational entropy because direct assessment of configurational entropy is not easily obtainable. The well-known VTF equation, which applies to many metastable equilibrium supercooled liquids, can be obtained if a hyperbolic temperature dependence^{6,17} of the configurational heat capacity, i.e. $C_{p \text{ conf}}(T) = K/T$, is assumed where K is a constant,

$$\tau = \tau_0 \exp\left(\frac{CT_K/K}{T - T_K}\right) = \tau_0 \exp\left(\frac{DT_0}{T - T_0}\right) \quad (3)$$

and T_0 denotes the zero molecular mobility temperature and has the same physical meaning as the Kauzmann temperature, T_K . D is the strength parameter.

As discussed in the literature,^{18–22} the molecular relaxation time constant of a nonequilibrium glass can be calculated from the configurational entropy of the metastable equilibrium glass via the fictive temperature, T_f , using the AGV^{17,23} equation:

$$\tau(T, T_f) = \tau_0 \exp\left(\frac{DT_0}{T - (T/T_f)T_0}\right) \quad (4)$$

The fictive temperature, by definition,⁶ is a temperature at which a metastable equilibrium glass has the same thermodynamic properties (S , H , etc.) as a nonequilibrium glass at

(16) Townley, E.; Roden, P. High-performance liquid chromatographic analysis of griseofulvin in drug substance and solid dosage forms: Separation of impurities and metabolites. *J. Pharm. Sci.* **1980**, *69*, 523–526.

- (17) Hodge, I. M. Enthalpy relaxation and recovery in amorphous materials. *J. Non-Cryst. Solids* **1994**, *169*, 211–266.
- (18) Tool, A. Q.; Eichlin, C. G. Variations caused in the heating curves of glass by heat treatment. *J. Am. Ceram. Soc.* **1931**, *14*, 276–308.
- (19) Tool, A. Q. Relation between inelastic deformability and thermal expansion of glass in its annealing range. *J. Am. Ceram. Soc.* **1946**, *29*, 240–253.
- (20) Ritland, H. N. Limitations of the fictive temperature concept. *J. Am. Ceram. Soc.* **1956**, *39*, 403–406.
- (21) Narayanaswamy, O. S. Model of structural relaxation in glass. *J. Am. Ceram. Soc.* **1971**, *54*, 491–498.
- (22) Scherer, G. W. Use of the Adam-Gibbs equation in the analysis of structural relaxation. *J. Am. Ceram. Soc.* **1984**, *67*, 504–511.
- (23) Hodge, I. M. Effects of annealing and prior history on enthalpy relaxation in glassy polymers. 6. Adam-Gibbs formulation of nonlinearity. *Macromolecules* **1987**, *20*, 2897–2908.

Table 1. Summary of the Physical Meaning of Isothermal and Non-Isothermal Apparent Activation Energies^{29,30}

nucleation mechanism	reaction order (n)	apparent E_a^a	
		isothermal	non-isothermal
continuous	$m + 1$	$(E_a^N + mE_a^G)/(m + 1)$	$(E_a^N + mE_a^G)/(m + 1)$
fixed number	m	E_a^G	E_a^G
site saturated	m	$(E_a^N + mE_a^G)/m$	E_a^G

^a The superscripts N and G refer to nucleation and one-dimensional growth, respectively.

temperature T . The fictive temperature can be calculated based on heat capacity data for fresh glasses⁶ and by combining enthalpy relaxation data for annealed glasses.¹³ For most freshly prepared glasses, the configurational entropy below T_g changes insignificantly with temperature, and T_f could be well approximated by T_g .

Crystallization Kinetics. Crystallization kinetics of amorphous materials has been extensively studied in ceramics and glasses, because crystallization leads to dramatic changes to their mechanical, optical, electrical, magnetic, and other properties. Crystallization usually involves two steps, nucleation and crystal growth. The kinetics of crystallization can be derived from the assumptions of nucleation, crystal growth, and termination of growth when two crystals meet. Generally, crystallization kinetics is well described by the Johnson–Mehl–Avrami (JMA) equation:^{24–27}

$$\alpha(t) = 1 - \exp\left[-\int_0^t g\left[\int_\tau^t Y(\Theta) d\Theta\right]^m I(\tau) d\tau\right] \quad (5)$$

where α is the conversion at time t , i.e., the fraction crystallized, $Y(\Theta)$ represents the growth rate in one of the m dimensions, $I(t)$ represents the rate of nucleation, and g is a geometric factor. The JMA equation has been further simplified:²⁸

$$\alpha = 1 - \exp[-(k(t - t_0))^n] \quad (6)$$

where k is the apparent crystallization rate constant (time^{-1}), t is the time, t_0 is the induction time, and n is the reaction order that depends on the nucleation mechanism and the number of dimensions, m , in which crystal growth is occurring. In this simplification, the overall rate constant is an average value of the rate constants for nucleation and crystal growth depending on the nucleation mechanism.

Various nucleation mechanisms are known, such as continuous nucleation, fixed number of nuclei, and site-saturated nucleation.²⁹ In continuous nucleation, the nuclei are formed continuously during the whole process of crystallization. In the second case, the number of nuclei does not change with changes in the experimental conditions, because the rate of nucleation is much smaller than the rate of crystal growth, and crystal growth proceeds on the preexisting nuclei. This process often occurs when a system is intentionally seeded. Site-saturated nucleation is similar to fixed number of nuclei, except that the number of nuclei depends on the experimental temperature. In this case, nucleation usually has much higher activation energy than growth. Therefore, once nuclei are formed, their growth proceeds quickly until the amorphous phase has completely crystallized. Further nucleation during growth is negligible because of its relatively slow nucleation rate.

The nucleation mechanism can be derived from a kinetic study. Assuming that both the rate of nucleation and the rate of crystal growth obey the Arrhenius equation, Woldt³⁰ derived a relationship for activation energies of isothermal and non-isothermal crystallization, based on the above three nucleation mechanisms. These relationships can be used to check the nucleation mechanism, if the activation energy for isothermal and non-isothermal crystallization is known. Table 1 summarizes the relationship.^{29,30} In general, the apparent activation energy, E_a , is the arithmetic mean of the activation energies for crystal growth in each dimension, E_a^G , and/or the activation energy for nucleation, E_a^N , depending on whether or not nucleation occurs. The reaction order, n , is equal to $m + 1$, if nucleation is continuous, or is otherwise equal to m , where m is the dimensionality of crystal growth. Isothermal and non-isothermal studies give the same apparent activation energy in the cases of continuous nucleation and fixed number of nuclei, whereas the apparent activation energy is different in site-saturated nucleation.

Kissinger^{31,32} analysis can be used to obtain the non-isothermal apparent activation energy:

$$\ln\left(\frac{q}{T_p^2}\right) = C - \frac{E_a}{RT_p} \quad (7)$$

where q is the heating rate, T_p is the peak temperature of crystallization, R is the gas constant, and C is a constant.

- (24) Avrami, M. Kinetics of phase change. I. General theory. *J. Chem. Phys.* **1939**, 7, 1103–1112.
- (25) Avrami, M. Kinetics of phase change. II. Transformation-time relations for random distribution of nuclei. *J. Chem. Phys.* **1940**, 8, 212–224.
- (26) Avrami, M. Kinetics of phase change. III. Granulation, phase change, and microstructure. *J. Chem. Phys.* **1941**, 9, 177–184.
- (27) Johnson, W. A.; Mehl, R. F. Reaction kinetics in processes of nucleation and growth. *Trans. Am. Inst. Min. Metall. Eng.* **1939**, 135, 416–442.
- (28) Maffezzoli, A.; Kenny, J. M.; Torre, L. On the physical dimensions of the Avrami constant. *Thermochim. Acta* **1995**, 269/270, 185–190.
- (29) Schmitt, E. A.; Law, D.; Zhang, G. G. Z. Nucleation and crystallization kinetics of hydrated amorphous lactose above the glass transition temperature. *J. Pharm. Sci.* **1999**, 88, 291–296.
- (30) Woldt, E. The relationship between isothermal and nonisothermal description of Johnson–Mehl–Avrami–Kolmogorov kinetics. *J. Phys. Chem. Solids* **1992**, 53, 521–527.
- (31) Kissinger, H. E. Variation of peak temperature with heating rate in differential thermal analysis. *J. Res. Natl. Bur. Stand.* **1956**, 57, 217–221.
- (32) Kissinger, H. E. Reaction kinetics in differential thermal analysis. *Anal. Chem.* **1957**, 29, 1702–1706.

Correlation of Molecular Mobility to Crystallization.

Diffusivity is related to viscosity, which is again related to molecular relaxation time. Their relationship is illustrated by the Stokes–Einstein equation for molecular translation and the Debye equation for molecular rotation, respectively:

$$D_{\text{trans}} = \frac{k_B T}{6\pi\eta r} \quad (8)$$

$$D_{\text{rot}} = \frac{k_B T}{8\pi\eta r^3} \quad (9)$$

where D_{trans} and D_{rot} are translational and rotational diffusivities, respectively. η is the viscosity, r is the size (radius) of the spherical molecule, k_B is the Boltzmann constant, and T is absolute temperature. In both cases the diffusivity is proportional to the temperature, and inversely proportional to the viscosity. Viscosity is proportional to the molecular relaxation time, τ . Zografi and co-workers⁹ have described the correlation between the rate of a process and diffusivity as follows:

$$\frac{k_1}{k_2} = \left(\frac{D_1}{D_2} \right)^\xi \quad (10)$$

where k_1 and k_2 are the rate constants at two different temperatures, T_1 and T_2 , respectively, and D_1 and D_2 are the corresponding diffusivities. ξ is termed the correlation index, where $0 \leq \xi \leq 1$, and expresses the extent of correlation between the diffusion and the rate of a reaction. When $\xi = 1$ the rate of the reaction is entirely dependent on the diffusion of the reactants or products. When $\xi = 0$, the diffusion process is not rate limiting. However, diffusion is often partially rate limiting and thus ξ lies between 0 and 1. The relationship between the rate of a reaction and molecular mobility can be derived, once we know how diffusivity is related to molecular mobility. The application of the Stokes–Einstein equation or the Debye equation⁹ gives

$$\frac{k_1}{k_2} \approx \frac{D_1}{D_2} = \left(\frac{T_1 \eta_2}{T_2 \eta_1} \right)^\xi = \left(\frac{T_1 \tau_2}{T_2 \tau_1} \right)^\xi \quad (11)$$

This equation may apply only qualitatively to reactions in the amorphous state, because the Stokes–Einstein and Debye equations are derived for spherical molecules in the liquid state and may not be applicable to amorphous supercooled liquid or glasses. In spite of this concern, eq 11 does illustrate the relationship between the rate of a reaction and molecular mobility. A more appropriate correlation might be derived from free volume theory. If we combine Doolittle's viscosity equation³³ and Turnbull's equation³⁴ on molecular transport in amorphous glass based on free volume concepts,^{35,36} we

(33) Doolittle, A. K. Studies in Newtonian flow. II. The dependence of the viscosity of liquids on free-space. *J. Appl. Phys.* **1951**, *22*, 1471–1475.

(34) Cohen, M. H.; Turnbull, D. Molecular transport in liquids and glasses. *J. Chem. Phys.* **1959**, *31*, 1164–1169.

(35) Turnbull, D.; Cohen, M. H. Free-volume model of amorphous phase glass transitions. *J. Chem. Phys.* **1961**, *34*, 120–125.

(36) Turnbull, D.; Cohen, M. H. On free-volume model of liquid-glass transitions. *J. Chem. Phys.* **1970**, *52*, 3038–3041.

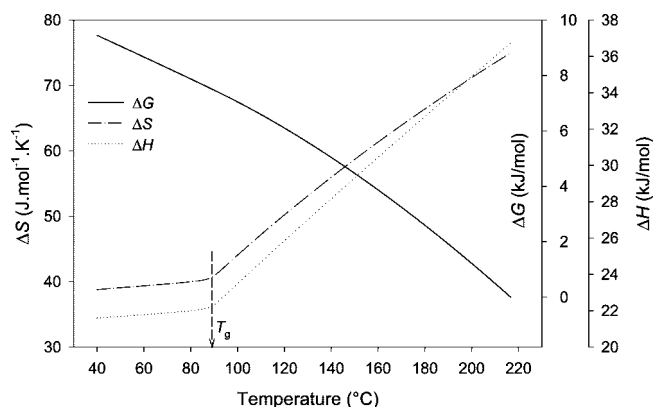


Figure 2. The excess thermodynamic quantities (ΔS , ΔH , and ΔG) of amorphous griseofulvin as compared to the crystalline state.

can relate the diffusivity to the viscosity in the amorphous state as follows:

$$\eta = A \exp(bv_0/v_f) \quad (12)$$

$$D = \frac{1}{3} \left(\frac{3k_B T}{m} \right)^{1/2} \exp(-\gamma v^*/v_f) \quad (13)$$

$$D = BT^{1/2}/\eta^\delta \quad (14)$$

where A , b , γ , B , and δ are constants ($\delta = \gamma v^*/bv_0$, $B = A^\delta (a^2 k_B/3m)^{1/2}$), a is the molecular diameter, k_B is the Boltzmann constant, and m is the mass of the molecule, while v_0 , v_f and v^* are the molecular volume at 0 K, the free volume, and the critical free volume for molecular diffusion. The constant δ is close to unity in most cases but it can also be applied to systems for which δ is less than 1. Equation 14 differs from the Stokes–Einstein and Debye equations in the square root temperature dependence of diffusivity, which is more realistic in the supercooled liquid state, according to Cohen and Turnbull.³⁴ From eqs 10 and 14, the relationship between molecular mobility and rate of a reaction can be derived, assuming $\delta = 1$:

$$\frac{k_1}{k_2} = \left(\frac{D_1}{D_2} \right)^\xi = \left(\frac{T_1}{T_2} \right)^{\frac{\xi}{2}} \left(\frac{\tau_2}{\tau_1} \right)^\xi \quad (15)$$

Results and Discussion

Thermal Stability. Griseofulvin was found to be stable chemically at 223 °C when assayed by HPLC. Even after holding at 223 °C for 3 h, the recovery of griseofulvin remained as high as 99.5%. The chromatograms of the stressed samples were similar to those of the original samples.

Thermodynamics of Amorphous Phase. The excess thermodynamic quantities of amorphous griseofulvin shown in Figure 2 were calculated using heat capacity data (not shown) and thermal properties of crystalline and amorphous griseofulvin given in Table 2. As is expected, the amorphous phase has higher enthalpy, entropy and free energy than the crystalline phase. Both ΔS and ΔH also show abrupt change in slope at the glass transition temperature, T_g . The ΔG line is continuous, which is consistent with the definition of a second order phase transition. Below T_g , the temperature

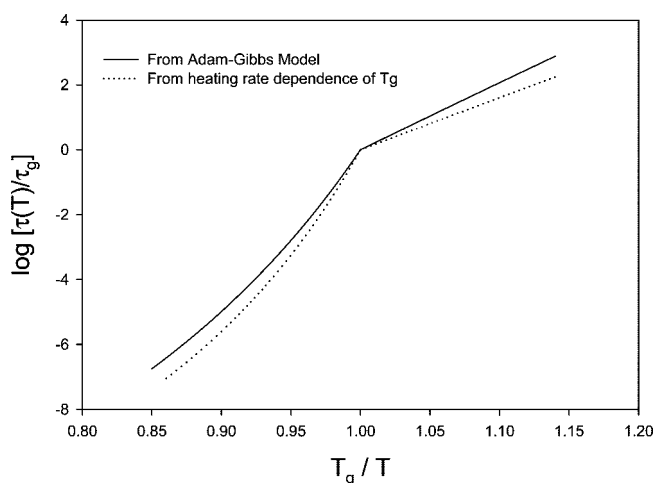
Table 2. Summary of the Thermal Properties of Crystalline and Amorphous Griseofulvin

parameter	values
T_m (°C)	216.7
ΔH_m (kJ·mol ⁻¹)	36.7
ΔS_m (J·mol ⁻¹ ·K ⁻¹)	74.9
T_g (°C)	88.9
T_K (°C)	-7.5
D	13.4
$T_m - T_g$ (°C)	127.8
$T_g - T_K$ (°C)	96.4
$S_c^{T_g}$ (J·mol ⁻¹ ·K ⁻¹)	41.7
$\Delta C_p^{T_g}$ (J·mol ⁻¹ ·K ⁻¹)	112.9

dependences of both ΔS and ΔH are much smaller than those above T_g , indicating that much of the excess entropy and enthalpy is trapped in the glassy state. The positive ΔG results from the fact that the ΔH term is larger than the $T\Delta S$ term ($\Delta G = \Delta H - T\Delta S$) because both ΔH and ΔS terms are positive. Hence, the thermodynamic driving force for crystallization of the amorphous form is its higher enthalpy. This thermodynamic driving force for crystallization is comparable to other small pharmaceutical molecules.¹² The kinetic basis for the propensity of griseofulvin crystallization is related to the excess entropy and its impact on molecular mobility as described by the Adam–Gibbs model. Amorphous griseofulvin has an excess entropy value of approximately 42 J·mol⁻¹·K⁻¹ at T_g . This is higher than other easily crystallizable compounds such as acetaminophen of 29 J·mol⁻¹·K⁻¹ but similar to compounds such as fenofibrate of 44 J·mol⁻¹·K⁻¹ and nifedipine of 47 J·mol⁻¹·K⁻¹, which exhibit intermediate crystallization tendencies.^{12,13} Thus, this property indicates at least intermediate crystallization tendency of griseofulvin. In addition, its configurational heat capacity at T_g of 113 J·mol⁻¹·K⁻¹ is close to 97 J·mol⁻¹·K⁻¹ for amorphous acetaminophen and 114 J·mol⁻¹·K⁻¹ for amorphous nifedipine, which also serves as an initial indicator of crystallization tendency.¹³ Therefore, amorphous griseofulvin is expected to have a crystallization tendency intermediate between acetaminophen and nifedipine based on configurational entropy and configurational heat capacity.

Molecular Mobility of Amorphous Phase. The Adam–Gibbs model and heat capacity data were used to derive the following parameters for amorphous griseofulvin: $T_g = 88.9$ °C, $D = 13.4$, and $T_K = -7.5$ °C. The relaxation time constant of griseofulvin glass ranges from 100 s at T_g to 10^{5.3} s at $T_g - 50$ °C. For comparison, the relaxation time constants at $T_g - 50$ °C for amorphous nifedipine, fenofibrate, and acetaminophen are 10^{6.2} s, 10⁷ s, 10^{7.5} s, respectively.^{12,13} These numbers suggest that griseofulvin glass has a higher molecular mobility, which also enhances its crystallization tendency.

The heating rate dependence of the glass transition temperature gave an apparent activation energy of 64.75 kJ/mol, $D = 9.6$, and $T_K = 14.3$ °C. Figure 3 presents a comparison between the molecular relaxation times generated

**Figure 3.** Molecular relaxation time of amorphous griseofulvin above and below T_g . Solid and dotted lines represent assessment from two different methods (see text). τ_g is the relaxation time at T_g (throughout this text).

by these two methods. Although the two sets of parameters were quite different, the molecular relaxation time constant plots appear remarkably similar. The small difference in the plots may arise from the substitution of excess entropy for configurational entropy. Excess entropy may contain contributions from nonconformational sources such as changes in vibrational frequencies or anharmonic vibrations as discussed by Goldstein.³⁷ Griseofulvin molecules are tightly packed in the crystal lattice and it is expected that the vibrations in this crystalline state are much more hindered than in the amorphous state. Therefore, the vibrational (nonconfigurational) contribution to the excess entropy of amorphous griseofulvin may not be negligible. Situations do exist where relaxation time based on this approach do not agree with that by other methods, e.g., sucrose.⁶ However, in other cases the relaxation time constants determined by different methods agree quite well.¹³

Given the similarity of the two curves in Figure 3, the Adam–Gibbs based molecular relaxation time will be employed for the subsequent discussion.

Crystallization. Amorphous griseofulvin was found to crystallize at temperatures above and below its glass transition temperature. Above T_g , crystallization proceeds at a considerable rate. Even at $T_g + 20$ °C (110 °C), crystallization is complete in about 16 h, although this rate is too small to be monitored *in situ* by DSC.

Figures 4 (a) and 4(b) show typical DSC profiles for isothermal and non-isothermal crystallization of amorphous griseofulvin, respectively. For both isothermal and non-isothermal crystallization, the rate of crystallization, as indicated by the magnitude of the heat flow, increases with conversion to the crystalline phase.

(37) Goldstein, M. Viscous liquids and the glass transition. V. Sources of the excess specific heat of the liquid. *J. Chem. Phys.* **1976**, *64*, 4767–4774.

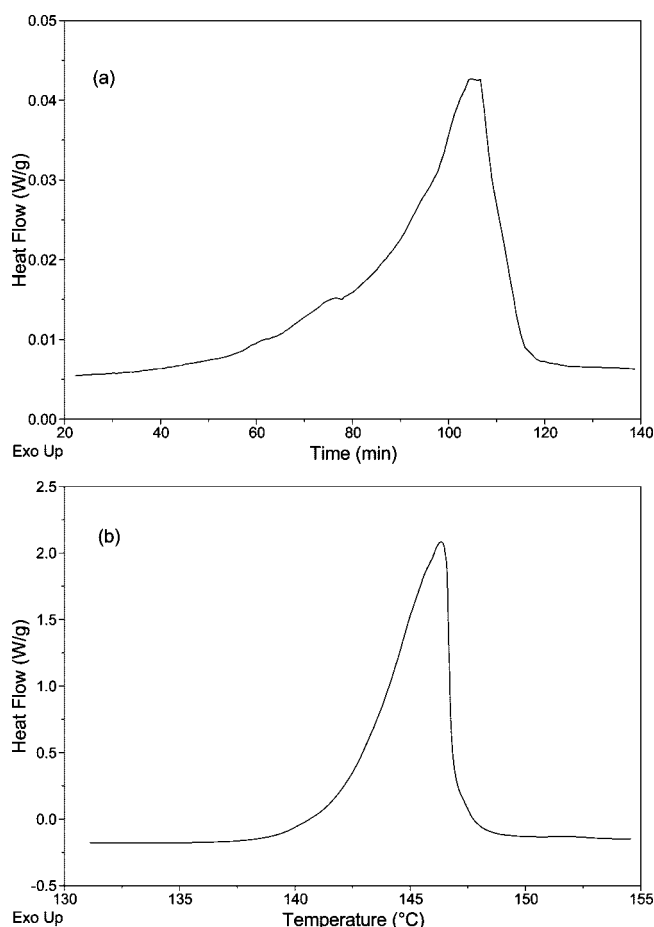


Figure 4. Typical DSC profiles for crystallization of amorphous griseofulvin (a) isothermally at 134 °C and (b) non-isothermally at 5 °C/min.

The crystallization profiles under isothermal conditions above and below T_g are shown in Figure 5. Note that crystallization occurs at a significant rate even at temperatures well below the T_g . For example, at $T_g - 30$ °C (60 °C), half of the amorphous phase crystallized in less than one month. This behavior makes amorphous griseofulvin a convenient model for investigating the relationship between the rate of crystallization and molecular mobility.

The griseofulvin molecule (Figure 1) is rigid and polar, and the crystalline phase is closely packed with a density of 1.42 g/cm³ compared to typical molecular crystals which have densities of ~1.3 g/cm³. As a result, griseofulvin has a high melting point ($T_m \sim 217$ °C) and heat of fusion as given in Table 2. Griseofulvin molecules are relatively small and compact and therefore have relatively high molecular mobility in the amorphous state. The rigidity of the molecule also reduces the number of possible conformations leading to lower configurational entropy and suggesting a high probability of attaining the specific conformation required in the crystal lattice. High mobility and low configurational entropy both favor crystallization from the amorphous state.^{12,13} As a result, care must be taken when preparing amorphous griseofulvin.

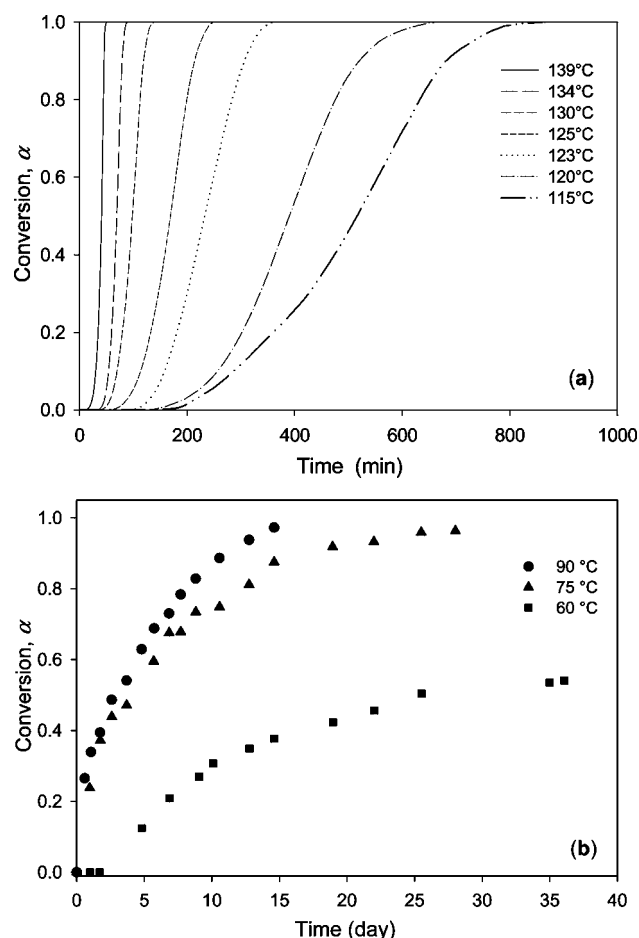


Figure 5. Crystallization profiles, conversion versus time, for isothermal crystallization of amorphous griseofulvin at temperatures (a) above its T_g and (b) at and below its T_g .

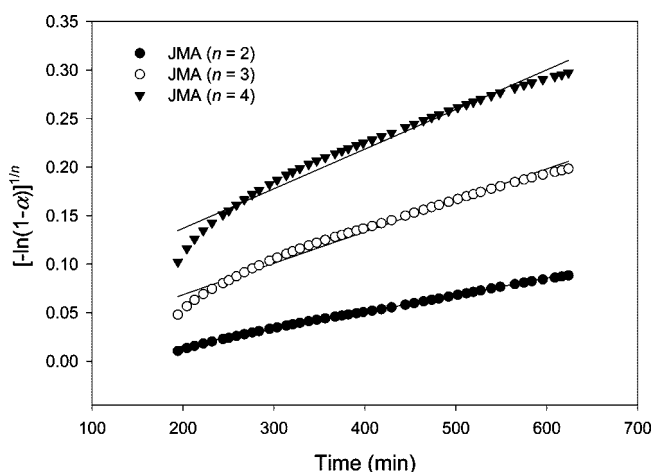


Figure 6. Johnson-Mehl-Avrami (JMA) plots for the crystallization of amorphous griseofulvin at 115 °C.

Comparison of the apparent E_a values from isothermal and non-isothermal studies combined with microscopic observations can be used to elucidate the nucleation mechanism.²⁹ Figure 6 shows the JMA plots for isothermal crystallization at 115 °C in the conversion range $\alpha < 0.8$. The JMA equation was converted to linear form for each possible

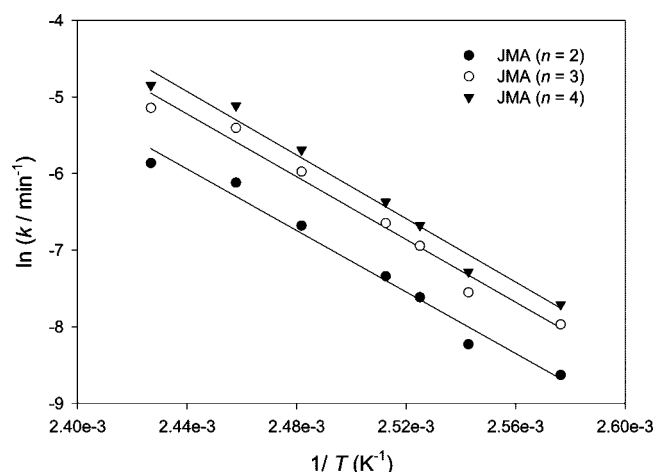


Figure 7. Arrhenius plots for the isothermal crystallization of amorphous griseofulvin above T_g . The rate constants were derived from fitting the data to three set of kinetic models: (●) second-order JMA, (○) third-order JMA, and (▼) fourth-order JMA.

reaction order, $n = 2, 3, 4$, respectively. The JMA plot with $n = 2$ gives a better fit than either the third or fourth order JMA plots. Similar situations occurred at other temperatures above T_g . All three models (JMA, $n = 2, 3$, and 4) give similar activation energies: 167, 170, and 172 kJ/mol for the second-, third-, and fourth-order models, respectively (Figure 7). A similar phenomenon was reported in a number of other cases,^{38,39} and it has been mathematically shown that processes following a single mechanism will give identical activation energy regardless of the model used to fit the data.⁴⁰

Therefore, based on curve fitting results, the second order JMA equation is considered the appropriate kinetic model for crystallization above T_g . Apparent rate constants at each temperature were then calculated from the fits to the second order JMA equation, and thus the isothermal crystallization process above T_g has an activation energy of 167 kJ/mol.

The crystallization profiles below T_g at 60 °C, 75 °C, and 90 °C were simply fitted to the second order JMA equation. The isothermal rate constants were derived from the fittings. An activation energy of 30.2 kJ/mol was obtained for crystallization below T_g , which is drastically smaller than the isothermal crystallization above T_g .

The non-isothermal apparent E_a for unseeded samples (Figure 8) is 184 kJ/mol, which is within experimental error of that from isothermal studies (167 kJ/mol), suggesting a continuous nucleation or fixed number of nuclei mechanism. A greater error was associated with the E_a of the seeded

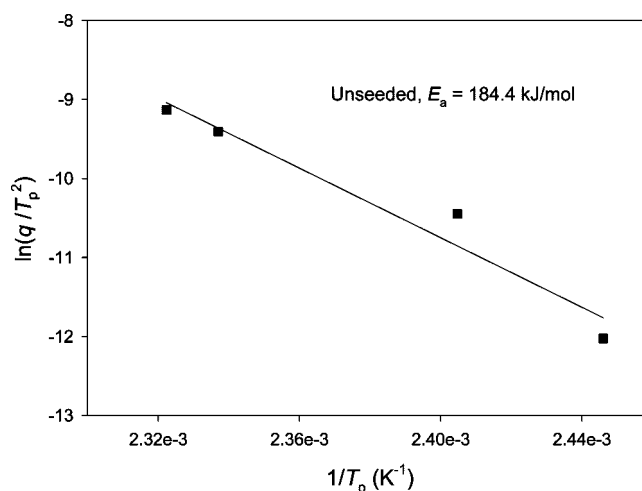


Figure 8. Kissinger plots for unseeded non-isothermal crystallization of amorphous griseofulvin.

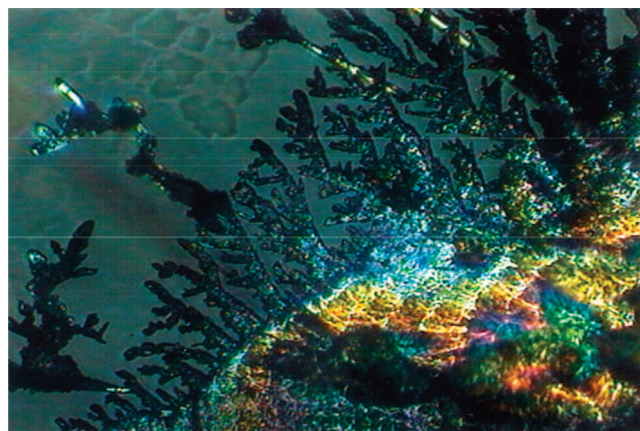


Figure 9. Hot stage micrographs of crystallized griseofulvin.

sample, and the activation energy could not be obtained with reasonable confidence. Therefore, distinction between the mechanisms of the continuous nucleation and of the fixed number of nuclei could not be made based on these two experiments. The greater error in the seed samples may be attributed to the inhomogeneity of the seeding process.

Figure 9 shows a hot stage micrograph of amorphous griseofulvin crystallized above T_g . Visually, the formation of the crystalline phase appeared to follow a two-dimensional dendritic growth, thereby implying a fixed number of nuclei mechanism.

Correlation between Crystallization Rate and Molecular Mobility. Molecular mobility has been suggested to be key determinant of the physical and/or chemical stability of amorphous phases. For any physical or chemical process, the molecules involved must take appropriate positions and orientations so that reaction can take place. Therefore, molecular motions, such as translation and rotation, are essential in any physical or chemical processes. In solution or in the melt, molecular translation and rotation are usually faster than the physical or chemical change itself so that the overall rate does not depend on diffusion of the reactant or product. However, in the solid state, molecular

(38) Byrn, S. R.; Pfeiffer, R. R. and Stowell, J. G. *Solid-State Chemistry of Drugs*, 2nd ed.; SSCI Inc: West Lafayette, IN, 1999; p 452.

(39) Zhou, D.; Schmitt, E. A.; Zhang, G. G.; Law, D.; Vyazovkin, S.; Wight, C. A.; Grant, D. J. W. Crystallization kinetics of amorphous nifedipine studied by model-fitting and model-free approaches. *J. Pharm. Sci.* **2003**, 92, 1779–1792.

(40) Zhou, D.; Grant, D. J. W. Model dependence of the activation energy derived from nonisothermal kinetic data. *J. Phys. Chem.* **2004**, 108A, 4239–4246.

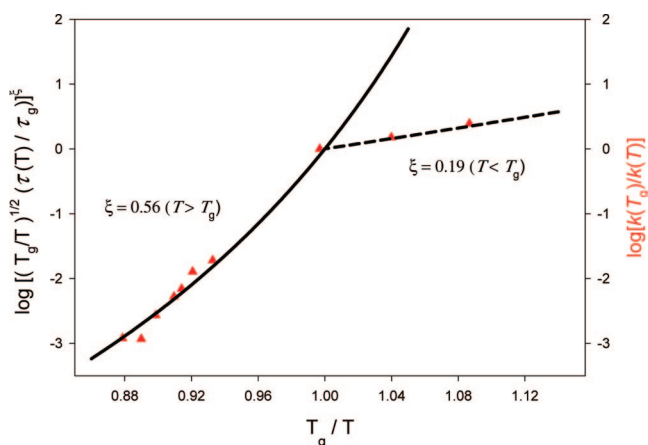


Figure 10. Correlation between the molecular relaxation time and the rate constants for crystallization of amorphous griseofulvin above and below its T_g . Triangles represent the experimental rate constant relative to that at T_g . The solid line represents correlated molecular relaxation time above T_g . The dotted line represents correlated molecular relaxation time below T_g .

diffusion is relatively slow and, in most cases, can be comparable to, or even slower than, the rate of reaction. It is likely that molecular motion becomes partially or completely rate limiting in solid-state reactions. One example is the curing reaction of resin,⁴¹ in which the viscosity increases due to cross-linking as the reaction proceeds and, as a result, the molecular mobility decreases and the apparent activation energy increases with time.

In the case of griseofulvin, Figure 10 shows the correlations between the molecular mobility and the rate constant for crystallization of amorphous griseofulvin at temperatures above and below its T_g . The extent of correlation shown in eq 15 as ξ was obtained from the slope of a plot of $\log k$ vs $\log(\sqrt{T}/\tau)$. The ordinate values for Figure 10 were then calculated using the ξ -values obtained above. The rate of crystallization shows partial correlation with molecular mobility ($\xi < 1$) at temperatures above and below T_g . Above T_g , the extent of correlation is about 0.56 while below T_g it is only about 0.19. As a comparison, if the molecular relaxation time based on the heating rate dependence of T_g were used, a correlation coefficient of 0.48 is obtained above T_g and 0.24 below T_g . Therefore, the qualitative picture of the correlation is similar regardless of method used to determine molecular mobility.

The incomplete correlation indicates that molecular motion is partially involved in the rate determining step, although it may also be the consequence of decoupling between molecular diffusion and viscosity.^{8,42,43} Another interesting

aspect of the correlation is the weaker dependence on molecular mobility in the glassy state than in the rubbery state. As temperature decreases, molecular motion slows down, and the rate of crystallization is expected to depend increasingly on the diffusion process. Thus, intuitively a stronger correlation is expected below T_g , which is the opposite of what was observed.

A possible explanation for this unanticipated result is a change in crystallization mechanism below T_g . Using eq 15 and substituting the terms with the following Arrhenius relationships, $\log k \propto -E_a^1/RT$ and $\log \sqrt{T}/\tau \propto -E_a^2/RT$, it can be shown that the correlation between rate of crystallization and molecular mobility (ξ), is equal to the ratio of the activation energies of the two processes. The activation energies of crystallization are 178.5 and 30.2 kJ/mol above and below T_g , respectively. The activation energies of mobility are 312.9 and 155.2 kJ/mol above and below T_g . If the activation energies for both quantities do not change with temperature, the correlation would not change. However, changes in the temperature dependence of molecular mobility are expected based on the glass dynamics (such as the Adam–Gibbs model). In the glassy state, the temperature dependence of molecular mobility is less than that in the rubbery state, i.e. a smaller E_a is expected for glasses. Therefore, based on the change of molecular mobility alone, a stronger correlation is expected between the crystallization rate and molecular mobility in the glassy state than in the rubbery state if the crystallization mechanism does not change. However, the activation energy of crystallization decreased approximately 6-fold, while that of the molecular mobility decreased roughly 2-fold from the rubbery to the glassy states, resulting in a less extent of correlation below T_g . The large difference in the activation energy suggests a change of the crystallization mechanism is possible when the T_g is crossed.

Although we do not have strong evidence to support this explanation, changes in crystallization behavior around T_g have been reported in the literature. Hikima et al.⁴⁴ studied the *o*-terphenyl system and observed that crystal growth near T_g and below abruptly increased orders of magnitude faster than expected from diffusion controlled growth. Most recently, Yu and co-workers identified a few similar pharmaceutical systems including indomethacin,⁴⁵ nifedipine,⁴⁶ and the ROY system.^{47,48} Many questions still remain to be answered, however, this glass-crystal mode of crystal growth appeared to be related to precursors in liquid and crystal

(41) Vyazovkin, S.; Wight, C. A. Isothermal and non-isothermal kinetics of thermally stimulated reactions of solids. *Int. Rev. Phys. Chem.* **1998**, *17*, 407–433.

(42) Fujara, F.; Geil, B.; Sillescu, H.; Fleischer, G. Translational and rotational diffusion in supercooled orthoterphenyl close to the glass transition. *Z. Phys. B* **1992**, *88*, 195–204.

(43) Ngai, K. L.; Magill, J. H.; PLazek, D. J. Flow, diffusion and crystallization of supercooled liquid: Revisited. *J. Chem. Phys.* **2000**, *112*, 1887–1892.

(44) Hikima, T.; Adachi, Y.; Hanaya, M.; Oguni, M. Determination of potentially homogeneous-nucleation-based crystallization in *o*-terphenyl and an interpretation of the nucleation-enhancement mechanism. *Phys. Rev. B* **1995**, *52*, 3900–8.

(45) Wu, T.; Yu, L. Origin of enhanced crystal growth kinetics near T_g probed with indomethacin polymorphs. *J. Phys. Chem. B* **2006**, *110*, 15694–15699.

structure.^{47,48} It is possible this is the case for griseofulvin although further detailed studies are necessary to unveil the nature.

Conclusions

The amorphous phase of griseofulvin has been characterized with respect to thermodynamic and molecular mobility both above and below T_g . Comparison of the thermodynamic

properties and molecular mobility between griseofulvin and other small molecules indicate a high crystallization tendency. Crystallization kinetics of amorphous griseofulvin from the rubbery and glassy states were followed and found fit to a second order JMA model with a 2-dimensional dendritic growth. The rate of crystallization partially correlates with molecular mobility but to different extents at temperatures above and below the glass transition temperature. The activation energy of crystallization decreases drastically in the glassy state compared with the rubbery state, suggesting a change of crystallization mechanism. Molecular mobility plays an important role in determining the crystallization rate but does not fully explain the rate of crystallization. Similar to previous observations, the strong crystallization tendency of amorphous griseofulvin can be accounted for by its moderate to small configurational entropy and relatively high molecular mobility.

MP800169G

-
- (46) Ishida, H.; Wu, T.; Yu, L. Sudden rise of crystal growth rate of nifedipine near T_g without and with polyvinylpyrrolidone. *J. Pharm. Sci.* **2007**, *96*, 1131–1138.
- (47) Sun, Y.; Xi, H.; Chen, S.; Ediger, M. D.; Yu, L. Crystallization near glass transition: transition from diffusion-controlled to diffusionless crystal growth studied with seven polymorphs. *J. Phys. Chem.* **2008**, *112*, 661–664.
- (48) Sun, Y.; Xi, H.; Ediger, M. D.; Yu, L. Diffusionless crystal growth from glass has precursor in equilibrium liquid. *J. Phys. Chem. B* **2008**, *112*, 661–664.